

Longitudinal tension and mechanical stability of a pressurized straw tube

L. Glonti, T. Enik, V. Kekelidze, A. Kolesnikov, D. Madigozhin*,
N. Molokanova, S. Movchan, Yu. Potrebenikov, S. Shkarovskiy
Joint Institute for Nuclear Research, 141980, Dubna, Russia

December 8, 2021

Abstract

For the development of charged particle detectors based on straw tubes operating in vacuum, a special measurement technique is required for the evaluation of their mechanical properties. A summary of the known equations that govern straw behavior under internal pressure is provided, and a new experimental method of a strained pressurized straw tube study is presented in this paper. The Poisson's ratio of the straw wall, which defines the stability conditions of a built-in tube, is measured for the NA62 spectrometer straw, and its minimum pre-tension is estimated.

keywords: straw tracker, straw tube, vacuum, pressure
PACS[2010] 29.40.Cs 29.40.Gx

1 Introduction

During the past few decades, a series of experiments in high-energy physics have been designed to investigate very rare decay modes of kaon (see, for example, [1, 2]). In particular, the purpose of NA62 experiment at CERN SPS [1] is to measure $K^+ \rightarrow \pi^+ \nu \bar{\nu}$ decay branching ratio of the order of

*Corresponding author. Email address: madigo@mail.cern.ch

10^{-10} with an uncertainty of 10%. It will be a test of the Standard Model and a probe to possible new physics. This is a challenging task, requiring an unprecedented precision of π^+ momentum measurement in order to reject the dominating background using the evaluation of event missing mass. This requires a precise measurement of the momentum and position of the charged particle.

A minimal material budget requirement in such experiments stimulates the development of gaseous particle detectors based on straw tubes containing gas under atmospheric pressure and operating in vacuum. These tubes maintain an internal overpressure of 1 atm, but higher overpressure may be desirable for a slower drift of electrons in the gas.

From the mechanics of a column, it is known that, if a compressive axial load is applied to a clamped thin-walled tube without overpressure, the load critical value F_{crit} for buckling is [3, 4]

$$F_{crit} = 4\pi^2 EJ/L^2. \quad (1)$$

where R is the straw radius, L is its length, and h is the thickness of the tube wall. Further, E is the Young's modulus and $J = \int \int y^2 dx dy = \pi R^3 h$ is a second moment of the cross-section of the tube wall. EJ is known as the object flexural rigidity. For an NA62 straw tube $F_{crit} \approx 0.5N$, which is a small value.

It should be considered that a large straw deviation may appear when this limit is approached [4]. A shift of a few millimeters of the tube axis with respect to the anode wire may cause an electric discharge and detector malfunction. Only axial tension guarantees the buckling prevention for a long straw tube, and it has been demonstrated earlier [4, 5] that an internal overpressure changes this necessary minimum tension.

Moreover, pre-tension is required to maintain the curvature caused by gravity to be small for a straw placed horizontally. For the given straw geometry and overpressure, the only parameter for the curvature control is the preliminary stretching force applied to the straw.

Therefore, estimation of the minimum pre-tension of the straw is necessary for any design of a straw tracker operating in vacuum. However, the calculations based on the published material properties of the straw wall are not sufficiently precise, because these properties depend on the batch of material. Therefore, an experimental procedure for the evaluation of material properties of a straw under operating conditions may be very useful.

The main purpose of this article is to present a new experimental method to estimate the minimum preliminary stretching force required to prevent the pressurized straw buckling and to limit its gravitational curvature.

2 Mechanics of a pressurized straw tube

The pressurized tube problem is not new in the industry, but it is not well-known in high-energy physics instrumentation. Therefore, we provide a summary of the known equations driving the behavior of straw tubes under internal pressure.

Only two stress directions are essential for the problem of a strained straw under internal pressure: the axial direction along the straw axis (\parallel) and the circumferential direction (\perp) tangent to the cylindrical surface of the straw in the plane normal to the axis. For a thin-walled tube ($h \ll R$), it can be demonstrated that straw circumferential (hoop) stress caused by the inner overpressure P is always $\sigma_{\perp} = \frac{PR}{h}$ [6]. The axial stress σ_{\parallel} depends on the conditions at the straw ends.

2.1 Pressurized tube with free closed ends

We will begin with the simple formulae derived in the isotropy approximation, when the material properties do not depend on the considered direction. If the internal pressure acts not only on the cylindrical shell of the tube but also on the free ends closed by airtight end plugs, a simple relation can be derived between the hoop stress σ_{\perp} and the free closed tube axial stress $\sigma_{\parallel}^{free} = \frac{P\pi R^2}{2\pi Rh} = \frac{PR}{2h} = \sigma_{\perp}/2$ (see [6] for cylindrical pressure vessel).

Hoop stress leads to the transverse strain of the material of the straw wall defining the direct contribution to the relative radius increasing $\epsilon_{\perp}^d = \sigma_{\perp}/E = \frac{PR}{Eh}$. For the typical straw tube $\epsilon_{\perp}^d \ll 1$; thus, this value may be used as a small parameter to determine the order of the considered contribution to a strain. The direct contribution to the axial relative elongation $\epsilon_{\parallel} = \frac{\Delta L}{L}$ for the free closed tube has the same first order: $\epsilon_{\parallel}^d = \sigma_{\parallel}^{free}/E = \frac{PR}{2Eh}$.

The Poisson effect leads to the shortening of the straw wall in the direction perpendicular to the corresponding direct strain. The Poisson ratio μ is defined as the ratio of the perpendicular relative shortening to the corresponding direct relative elongation. Thus, we have the first approximation

for a free closed tube.

$$\frac{\Delta L}{L} = \epsilon_{\parallel} = \epsilon_{\parallel}^d - \mu \epsilon_{\perp}^d = \frac{PR}{2hE}(1 - 2\mu) \quad (2)$$

$$\frac{\Delta R}{R} = \epsilon_{\perp} = \epsilon_{\perp}^d - \mu \epsilon_{\parallel}^d = \frac{PR}{2hE}(2 - \mu). \quad (3)$$

In the paper [7], the equation (2) has been observed to be sufficiently precise to the best of our knowledge of the material properties. The hoop strain formula (3) has been derived for the pressure vessel in [8].

In an experimental set-up employing straws in vacuum, straw ends are usually built into the rigid frame (built-in tube) [1]. For this case, the formulae (2, 3) in general are incorrect, since the pressure force applied to the built-in end is balanced by the rigid frame rather than by the axial tension of the wall.

However, there is a special case wherein a built-in tube and a free closed tube are equivalent. Further, it can be used to obtain the simplest estimation of the minimum preliminary tension required to prevent straw buckling in vacuum [9]. If a free closed pressurized straw is glued into a rigid frame that exactly fits the straw length enlarged by the overpressure (2), the frame does not apply any axial load to the built-in straw. If the frame requires a longer straw, an overall axial tension is applied to the straw ends ensuring the stability of the tube against buckling. Furthermore, no change occurs in the state of the straw wall if we connect the inner straw volume with the gas supply mounted in the frame.

Therefore, in order to prevent buckling, we require a minimum straw pre-tension ensuring the elongation (2) prior to the vacuum creation around the tube. The stress caused by straw preliminary tension T_0^{min} should be at least $\frac{T_0^{min}}{2\pi Rh} = E\epsilon_{\parallel} = \frac{PR}{2h}(1 - 2\mu)$, and the minimum pre-tension for buckling prevention is

$$T_0^{min} = P\pi R^2(1 - 2\mu). \quad (4)$$

2.2 Pressurized tube with built-in ends

We will assume the different material properties in the axial and circumferential directions (orthotropic approximation), which is quite usual for a straw wall material. For example, NA62 straws are made of Hostaphan[®] polyethylene terephthalate (PET) film. The film manufacturer reports the different values of transverse (transverse direction, TD) and longitudinal (machine

direction, MD) Young's moduli [10] (see Table 1). Therefore, the direct contribution to the relative radius change of straw becomes $\epsilon_{\perp}^d = \sigma_{\perp}/E_{\perp} = PR/(E_{\perp}h)$.

Owing to the Poisson effect, the hoop strain causes an axial strain of the opposite sign, and thus, the straw becomes shorter if the ends are not built-in. This imaginary relative change of the length is $\epsilon_{\parallel}^{\mu} = -\mu_{\perp}\epsilon_{\perp}^d$, where μ_{\perp} is the transverse (circumferential for the tube) Poisson's ratio. However, the straw ends are fixed, which indicates an appearance of the compensatory tension force ΔT and the corresponding axial stress $\Delta T/(2\pi Rh)$, which returns the straw to its initial length:

$$\frac{\Delta T}{2\pi Rh} = -E_{\parallel}\epsilon_{\parallel}^{\mu} = \mu_{\perp}P\frac{R}{h}\frac{E_{\parallel}}{E_{\perp}}. \quad (5)$$

From Maxwell's reciprocity theorem, the known relation $\mu_{\parallel} = \mu_{\perp}\frac{E_{\parallel}}{E_{\perp}}$ can be derived, where μ_{\parallel} is the axial Poisson's ratio [4]. Thus, the wall axial tension is

$$T = T_0 + \Delta T = T_0 + 2\mu_{\parallel}P\pi R^2. \quad (6)$$

The total force applied by a gas-filled straw in vacuum on the detector frame can be considered as an "effective tension" $T_P = T - P\pi R^2$, if the effect of external atmospheric pressure applied to the frame is calculated by ignoring all holes made for the gas supply into the straws. For this effective tension, we obtain

$$T_P = T_0 - (1 - 2\mu_{\parallel})P\pi R^2. \quad (7)$$

Poisson's ratio μ for plastics is usually less than 0.5. Thus, the vacuum around a straw leading to its inner overpressure diminishes T_P with respect to the straw pre-tension T_0 in spite of the increase in true straw tension T (6).

2.3 Lateral effect of internal pressure

We will evaluate the summary force applied by internal pressure to the wall of a curved tube. Ignoring the flexural rigidity, consider a short element of a slightly curved tube (Figure 1), limited by its two cross-sections normal to the curved axis. The absolute longitudinal tension force $|T_{AB}| = |T_{CD}| = |T|$ is a constant in this approximation, but the directions of T_{AB} and T_{CD} forces are defined by different slopes at the element ends.

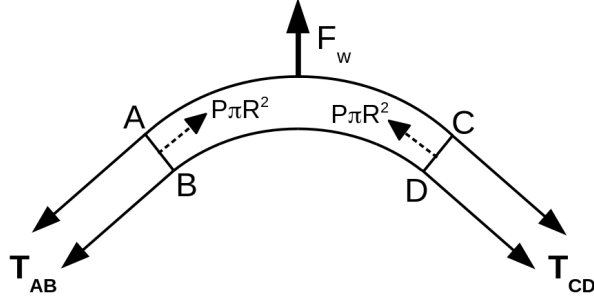


Figure 1: Forces applied to the curved tube element without flexural rigidity subject to internal pressure and axial tension

The area of the arched side of the wall (upper side in Figure 1) is larger than the area of the concave part. Consequently, a non-zero summary pressure force F_W applied to the wall appears, which is directed toward the arched side of the wall. Thus, the internal overpressure always attempts to increase the existing curvature of the tube.

The evaluation of summary pressure effect has been performed earlier in a few ways: an imaginary ideal piston at the boundary of the pressurized tube segment [11], the consideration of the forces applied to separated fluid contained within a tube element [12], and a direct integration of the pressure forces [4].

However, we can directly evaluate the pressure effect F_W without integration. For the given P , the summary force F_W depends only on the shape of the tube segment. Imagine an absolutely rigid shell consisting of a curved tube wall with additional transverse plugs closing the cross sections AB and CD tightly. A resultant force applied by inner overpressure to a closed rigid shell is always zero. Therefore, the total pressure force applied to the curved wall is equal, but with the opposite sign, to the vector sum of the pressure forces $P\pi R^2$ applied to the end plugs, which are perpendicular to the curved axis of the tube at the ends (see Figure 1). One of these forces is directed against T_{AB} , and the other against T_{CD} , which effectively diminishes the straw tension by the pressure-related force $P\pi R^2$.

Thus, the lateral dynamics of a curved tube element are defined by the effective tension $T_P = T - P\pi R^2 = T_0 - (1 - 2\mu_{||})P\pi R^2$, which replaces the true tension T in all the formulae describing a straw bending [12, 4, 5].

It is important to understand the physical difference between the effective tension T_P defining the straw bending phenomena and the tube wall tension T in the tensile strength formulae. Straw wall stress is normally increased owing to the internal overpressure, whereas the pressurized straw as an elastic body is effectively relaxed under the same conditions, and this relaxation is described by the pressure-dependent effective tension T_P behavior.

For $T_P < 0$, a summary transverse force pushes a curved straw element toward its arched side, and without flexural rigidity, the curvature increases until the tension (increased owing to the curved tube elongation) becomes equal to the pressure force everywhere along the tube: $T = P\pi R^2$.

From $T_P > 0$ and (7), we obtain the minimum longitudinal straw pretension T_0 to prevent buckling [4]

$$T_0^{min} = (1 - 2\mu_{||})P\pi R^2. \quad (8)$$

The same limit is defined by (4) derived in a different way.

2.4 Equilibrium of a horizontal straw

For a horizontally placed straw, we should ensure that the maximum vertical deviation (sagitta Sag) caused by gravitation is small. Consider a horizontal straw with built-in ends subject to vertically distributed gravitational load q and an internal overpressure P . We choose the origin of the axial coordinate x at the center of the straw. The axis of a straw lateral deviation y is directed downwards, thus $y(0) = Sag$. The linear gravitational load is $q = g\rho$, where ρ is the linear density of the straw and g is the gravitational acceleration.

The straw equilibrium equation for this case was derived in [4, 5]:

$$\frac{dF}{dx} = -EJ \frac{d^4 y}{dx^4} + T_P \frac{d^2 y}{dx^2} + q = 0, \quad (9)$$

where $\frac{dF}{dx}$ is a resulting force per unit of length, which is zero for the case of static equilibrium.

Straw ends in the NA62 spectrometer are glued into the frame (clamped). Therefore, the boundary conditions are $\frac{dy}{dx}(\pm \frac{L}{2}) = 0$ and $y(\pm \frac{L}{2}) = 0$. The symmetric solution ($y(x) = y(-x)$) for this static case is

$$y_s(x) = \frac{q}{2T_P} \left(\frac{L^2}{4} - x^2 + \frac{L}{k} \cdot \frac{\cosh(kx) - \cosh(kL/2)}{\sinh(kL/2)} \right), \quad (10)$$

where $k = \sqrt{\frac{T_P}{EJ}}$ (see [5]). Sagitta $y_s(0)$ is increased by the internal overpressure owing to the decrease in T_P (7).

2.5 Low-frequency oscillations

The interesting consequence of the pressure lateral effect is a straw vibration pressure dependence caused by the behavior of T_P used instead of string tension for straw transverse dynamics. For the case of oscillations, we should set $\frac{dF}{dx} = \rho \frac{d^2 y}{dt^2}$ instead of zero in (9). We will determine the solution in the form of $y(x, t) = y_s(x) + y_f(x, t)$, where $y_s(x)$ is a solution of the static equation (9). It leads to the wave equation

$$\rho \frac{d^2 y_f}{dt^2} = -EJ \frac{d^4 y_f}{dx^4} + T_P \frac{d^2 y_f}{dx^2} \quad (11)$$

set up by Lord Rayleigh [13].

We will determine the symmetric solution with fixed ends ($y_f(\pm \frac{L}{2}) = 0$) and with “pinned” boundary conditions ($\frac{d^2 y_f}{dx^2}(\pm \frac{L}{2}) = 0$). Such a simple solution is sufficient for the qualitative understanding of straw oscillations. These boundary conditions are satisfied for $y_f(x, t) = \cos((1+2n)\pi x/L) e^{i2\pi f t}$ with any integer n . For $n = 0$, the equation (11) results in $(2\pi f)^2 \rho = (\pi/L)^2 (EJ(\pi/L)^2 + T_P)$, and thus the lowest frequency of the straw vibration is [14]

$$f = \frac{1}{2L} \sqrt{\frac{EJ(\pi/L)^2 + T_P}{\rho}}. \quad (12)$$

Notably, the flexural rigidity of the straw results in an addition of $EJ(\pi/L)^2$ to the effective tension in (12). The frequency is decreased by the overpressure owing to the behavior of T_P (7).

2.6 Radius correction

T_P depends on the straw radius R considered so far as a constant value. However, R depends on P , whereas the radius of the built-in end plug remains unchanged. It leads to the formation of a radius transition zone on the tube wall near the straw end. However, the axial component of the pressure force applied to the transition zone is subtracted from the axial wall tension applied to the end plug. Therefore, for T_P calculation, we can consider the radius of the end plug to be equal to the pressure-dependent straw radius R .

The direct contribution of overpressure to the relative change of radius is $\frac{\sigma_{\perp}}{E_{\perp}} = \frac{PR}{E_{\perp} h}$, but if we consider the additional tension applied to the built-in ends, this term becomes $(1 - \mu_{\parallel} \mu_{\perp}) \frac{PR}{E_{\perp} h}$. Moreover, the applied pre-tension

T_0 diminishes the straw radius owing to the Poisson's effect. Therefore, we have

$$R = R_0(1 + (1 - \mu_{\parallel}\mu_{\perp})\frac{PR_0}{E_{\perp}h} - \frac{\mu_{\parallel}T_0}{E_{\parallel}2\pi R_0h}), \quad (13)$$

where R_0 is the initial radius of the straw. For T_P calculations, if $T_0 \approx 1$ kgf, the radius change (13) leads to the next-order correction in terms of the small parameter $\frac{PR}{Eh}$.

3 Poisson's ratio measurement

It can be observed from (8) that the straw buckling limit for a given overpressure is defined by the tube radius R and the Poisson's ratio μ_{\parallel} . The Poisson's ratio is typically not provided in the PET film specifications. The published independent measurements of μ are not related to the specific batch of material used in the straw tubes production for the given detector. Moreover, the straw production process may change some foil properties. Therefore, the μ_{\parallel} measurement procedure applicable to a welded straw is required in order to evaluate the minimum straw pre-tension for the specific detector design.

3.1 Straw specimens

Two straw specimens have been tested (see Table 1). The tubes are made of PET Hostaphan[®] foils using longitudinal welding [1]. The parameters of the foils can be found in the manufacturer specifications [10].

Table 1: Properties of the tested straws

Property	9.8-mm straw	18-mm straw
Diameter, mm	9.8(1)	18.0(1)
Length, m	2.10(1)	1.90(1)
Material density, g/cm ³	1.4(1)	1.4(1)
Wall thickness, μm	36(1)	54.4(8)
Tube linear density, g/m	1.55(12)	4.31(6)
E_{\parallel} , N/mm ²	4500(500)	4000(500)
E_{\perp} , N/mm ²	5000(500)	5500(500)

The first specimen (9.8-mm straw) is obtained from a party of approximately 7000 straws produced at the Joint Institute for Nuclear Research (Dubna) for NA62 spectrometer [1]. This 9.8-mm straw is coated inside the tube with two thin metal layers ($0.05\mu m$ of Cu and $0.02\mu m$ of Au) in order to provide electrical conductivity on the cathode and to improve the impermeability of the straw tube. The wall material volume density [10] is used to estimate the linear density of the 9.8-mm straw. The contributions of metal layers and the air mass inside the tube to linear density are negligible.

The second specimen (18-mm straw) is made of a thicker Hostaphan[®] film. In this case, the linear density of the tube has been measured by weighing, since the wall thickness is not strictly defined in the manufacturer specifications.

3.2 Test bench for studies of a strained straw under pressure

A special test bench (see Figure 2) has been manufactured in order to study the properties of a built-in straw with an initial pre-tension and an inner overpressure applied subsequently. The longitudinal force applied to the straw end $T_P = T - P\pi R^2$ is measured using a tensometer Tm based on a single-point aluminum load cell (Tedea-Huntleigh, model 1022) [15].

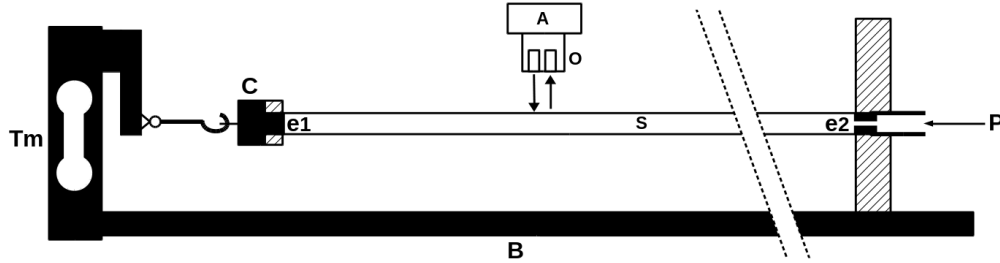


Figure 2: The test bench scheme: B – rigid basement; Tm – tensometer; e1 – closed end plug; e2 – end plug with a gas supply channel; C – end cap with a seal; P – pressure supply; S – straw; O – optical coupler; A - amplifier.

A straw specimen is closed on the tensometer side by the end plug e1 with the end cap C using glue for rigid sealing. The end cap C is connected to

the tensometer Tm using two flexible joints and a rigid rod. The other straw end contains a plug $e2$ with a gas supply channel. This straw end is glued into the solid support, which may be moved along the rigid basement B and fixed at a specific place in order to create a preliminary straw tension prior to the test. Subsequently, the pressure supply is opened, and the changing pressure values P are recorded together with the corresponding results of the tensometer measurement T_P (see points in Figure 3 and Figure 4A).

Straw oscillations are studied using the optical coupler O [1], which emits constant intensity infrared radiation and registers the radiation reflected from the straw wall. When the straw oscillations are mechanically excited, the registered radiation intensity is modulated by the changing distance to the straw wall. The obtained signal is amplified and sent to the oscilloscope with a fast Fourier transform function. The lowest frequency peak position is registered as the lowest frequency of the straw (points in Figure 4B).

The end cap C is slightly shifted down owing to its weight of $10 - 20$ gf. However, for the horizontal force $T_P > 300$ gf (assuming the cap weight of 25 gf), the vertical shift of the cup is less than 4 mm. It leads to the relative elongation of 2-m straw $\approx 10^{-4}$, which is much less than the minimum straw elongation caused by the tested preliminary tension (10^{-3}). Thus, the straw ends may be considered to be fixed during the test.

3.3 Effective tension and Poisson's ratio measurement

It is known that any material becomes nonlinear for a large stress, whereas the linear properties of the material are defined for zero-stress limit. However, on the built test bench, precision measurement becomes problematic for a low effective tension T_P . Therefore, we must consider the possible nonlinearity in such a way that the resulting μ_{\parallel} could be easily extracted for $T \rightarrow 0$.

Accordingly, we postulate a weak linear dependence of Poisson's ratio as a function of axial stress. For the fits of our experimental results, we use the tension-dependent value

$$\nu = \mu_{\parallel} - \frac{kT}{2\pi Rh} \quad (14)$$

instead of only μ_{\parallel} . Apart from the material nonlinearity, the coefficient k also absorbs the effect of the set-up deformation under tension and the next-order effects ignored in the formulae. Expression (14) provides a physically motivated interpolation and extrapolation of the measurement results, whereas in

order to compare the resulting Poisson's ratio with the other measurements, we can consider the measured μ_{\parallel} and ignore the stress-dependent term.

T and R variables in (14) depend on the Poisson's ratio value. Therefore, we implement an iterative procedure starting with a tension $T = T_0$, nominal straw radius $R = R_0$, and the starting Poisson's ratio value of $\nu = \mu_{\parallel}$. In each iteration, new T, ν, R values were calculated, and three iterations were sufficient for the precise calculation.

Two free parameters (μ_{\parallel} and k) describe the measured tensions and pressures satisfactorily. Figure 3 and Figure 4A show the measured effective tensions for the NA62 straw along with the result of their fit with the formula

$$T_P = T_0 - (1 - 2\nu)P\pi R^2. \quad (15)$$

The MINUIT [16] package and ROOT [17] interface were used to obtain the resulting parameter values and their fit errors.

Table 2: Poisson's ratio measurement results

	9.8 mm straw			18 mm straw		
	$k, \frac{\mu m^2}{gf}$	μ_{\parallel}	μ_{\perp}	$k, \frac{\mu m^2}{gf}$	μ_{\parallel}	μ_{\perp}
Central value	3.98	0.3055	0.3394	-2.89	0.2960	0.4070
Radius correction	0.43	0.0005	0.0006	0.92	0.0005	0.0007
Radius value	0.14	0.0083	0.0092	0.59	0.0039	0.0054
T_P scale	0.06	0.0099	0.0110	1.24	0.0088	0.0121
P scale	0.27	0.0094	0.0104	1.03	0.0084	0.0116
$\delta \frac{E_{\perp}}{E_{\parallel}}$	0	0	0.0306	0	0	0.0296
Systematic error	0.53	0.0160	0.0353	1.95	0.0128	0.0344
Statistical error	0.18	0.0005	0.0006	14.35	0.0150	0.0206
Total error	0.56	0.0160	0.0353	14.48	0.0197	0.0401

The fit to all the measured T_P values for the given straw is performed with a common set of free parameters and the same assumed measurement error. The error (± 3.6 gf for the 9.8-mm straw and ± 20.47 gf for the 18-mm straw) is defined in such a way that the resulting $\chi^2/ndf = 1$, in order to estimate the parameter statistical uncertainties.

The fit results and systematic uncertainty contributions are shown in Table 2. The coefficients of correlation between μ_{\parallel} and k are 0.991 for the

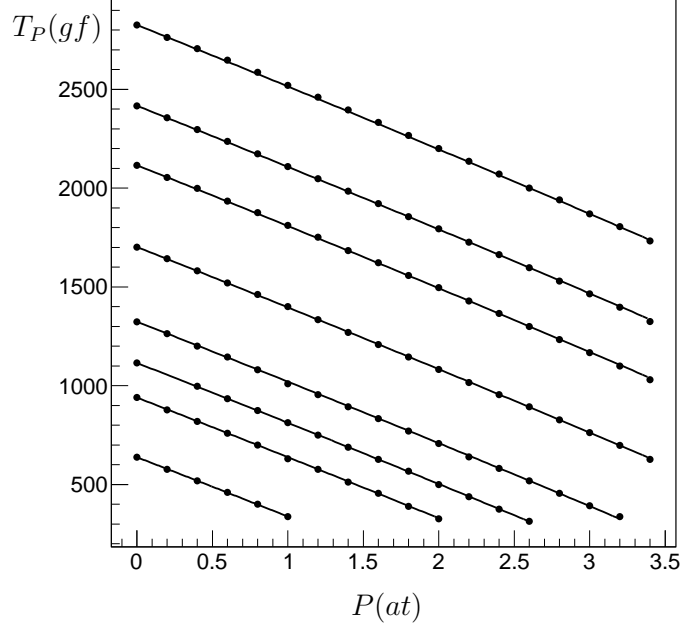


Figure 3: 9.8-mm straw effective tension T_P versus the overpressure P for different initial tensions $T_P(0)$. Circles – measurements; solid lines – fit by the formula (15).

9.8-mm straw and 1.000 for the 18-mm straw. Thus, for the second specimen, the presence of the non-zero term k is not confirmed.

The radius correction effect is considered, but it is also completely included in the systematic errors as a “Radius correction” contribution. The Gaussian width of the NA62 straw diameter distribution is approximately 0.03 mm, and the systematic shift of its central value from the nominal number has the same size [1]. Thus, considering a conservative value of the possible diameter systematic uncertainty of 0.1 mm for the tested specimens, we have obtained the “Radius value” contribution to the systematic error shown in Table 2. Moreover, the effects of a systematic scale shift of 5% on both the measured effective tension and measured pressure are considered as independent contributions (“ T_P scale” and “ P scale”) to the systematic errors.

Considering the manufacturers information about Young's moduli (see Table 1), the μ_{\perp} central values shown in Table 2 have been extracted as $\mu_{\perp} = \mu_{\parallel} \frac{E_{\perp}}{E_{\parallel}}$. Their uncertainties depend on the error of the modules ratio, which may be approximately estimated from the significant digits of the provided values as $\delta \frac{E_{\perp}}{E_{\parallel}} \approx 0.1$.

Typically, the reported Poisson's ratio values for the oriented PET films are 0.37-0.44 [18], and thus, the obtained μ_{\perp} values are consistent with them. However, the resulting μ_{\parallel} is approximately 0.3, which may be a specific property of Hostaphan[®] foil or the consequence of the production of straw tube using longitudinal welding [1].

4 Oscillation frequency measurements

The oscillation frequency measurement was the last test of the straw tensions performed on the assembled NA62 spectrometer modules [1]. The same test has been repeated on the present test bench for a qualitative verification of the pressure effect.

The length of the tube on the test bench is defined by the position of the movable support and the end cup C position. Unfortunately, when a straw tension is applied to the end cup fixed on the short rod with flexible joints, an effective oscillator is formed with a frequency close to the measured frequency of straw. Therefore, using this test bench, only a qualitative understanding of straw oscillations can be obtained using the simple frequency formula (12).

The results of the lowest frequency measurements are shown in Figure 4B along with the corresponding calculation results based on (12). The error bars show the frequency uncertainty of 1 Hz defined by the width of the observed spectrum peaks.

The prediction (12) for the 9.8-mm straw satisfactorily describes the measurement results in the vicinity of NA62 design parameters ($T_0 = 1500$ gf, $P = 1$ at). However, the overall discrepancy reaches 2 Hz, which is more than the measurement precision. Nevertheless, the obtained qualitative description of the straw vibration confirms that the lowest frequency of the straw is significantly diminished by the internal overpressure in spite of the increase in straw wall stress according to (6).

5 Minimum straw pre-tension evaluation

We can use the obtained Poisson's ratio to evaluate the minimum straw pre-tension T_0 in the straw-based NA62 spectrometer operating in vacuum [1].

There are two requirements for T_0 . The buckling limit $T_P > 0$ (where T_P is calculated from (15) for $P = 1$ at) is defined by the Poisson's ratio and the straw radius. The flexural rigidity contribution (1) to the buckling prevention is small for the long NA62 straw and may be included into the safety margin. Moreover, the experimental design requirements define the gravitational deviation (sagitta) limit for a horizontal straw. Sagitta $Sag = y_s(0)$ calculated from (10) depends on the effective tension, flexural rigidity, and straw length.

The sagitta requirement $Sag < 100 \mu\text{m}$ of NA62 [1] cannot be satisfied using a reasonable pre-tension for the complete 2.1-m straw. Hence, special supporting spacers dividing each straw into three equal parts are implemented in the NA62 spectrometer [1]. These spacers fix a straw only in one of the lateral directions, and thus, they do not change the small buckling critical load value (1) ignored in this study.

Straw symmetry near each spacer ensures that the boundary conditions of (10) are satisfied. Hence, we use this solution with $L = 0.7$ m in order to calculate the sagitta.

The results of the sagitta calculation and buckling limit estimations are shown in Figure 5A for the 9.8-mm straw in the NA62 spectrometer. The corresponding results for the 18-mm straw, assuming the same straw length of 70 cm, are shown in Figure 5B for comparison.

Apart from the most probable sagitta values and buckling limits, the worst cases are also shown in Figure 5. The worst case for each straw corresponds to ν (14) central value diminished by the tripled total uncertainty evaluated for each T_0 from the measured μ_{\parallel} and k considering their correlation. All other parameters for this worst-case scenario are considered at their uncertainty limits leading to the largest sagitta and the easiest buckling.

It can be observed from Figure 5 that, for the NA62 spectrometer, a straw pre-tension value above 900 gf guarantees $Sag < 100 \mu\text{m}$ (NA62 requirement), whereas the worst case of the buckling limit is below 400 gf. Thus, both the NA62 nominal straw pre-tension of 1.5 kgf and the factual minimum pre-tension (≈ 1.2 kgf) [1] have a good safety margin.

However, if the 18-mm straw is used in the same detector design, the minimum T_0 would be defined by the increased buckling limit above 1.15 kgf

with a small safety margin, whereas the gravitational sagitta will be always below $100\text{ }\mu\text{m}$ for the pre-tension above the buckling limit.

Conclusions

A new technique for the study of mechanical properties of straw tubes subjected to inner pressure and longitudinal tension has been tested using a specially built test bench. It includes the measurement of Poisson's ratio of a straw wall, which defines the buckling limit of a straw with a given radius under a definite inner overpressure.

The axial Poisson's ratio μ_{\parallel} for Hostaphan[®] foil is measured for two specimens under the conditions close to those of a detector operating in vacuum. The lateral Poisson's ratio μ_{\perp} is evaluated using the elasticity moduli in two directions provided by the foil producer. The spectra measurements of straw oscillations qualitatively confirm the effective tension predictions based on the measured μ_{\parallel} .

The minimum pre-tension requirement for the NA62 spectrometer is re-evaluated based on the measurement results. The obtained limit confirms the detector design pre-tension with a safety margin of approximately 600 gf. The tested technique can be used for the development of future straw trackers.

References

- [1] F. Hahn, et al., Na62: Technical design document, Tech. rep., CERN, Geneva, na62-10-07 (2010).
URL <https://cds.cern.ch/record/1404985/files/NA62-10-07.pdf>
- [2] A. Buonauro, SHiP: a new facility with a dedicated detector for studying ν_{τ} properties and nucleon structure functions, PoS DIS2016 (2016) 260. [arXiv:1609.04860](https://arxiv.org/abs/1609.04860).
- [3] S. Timoshenko, J. Gere, Theory of elastic stability, McGraw-Hill, 1961.
- [4] A. Catinaccio, Pipes under internal pressure and bending, Tech. rep., CERN, Geneva, pH-EP-Tech-Note-2009-004 (2010).

- [5] P. Wertelaers, Static behaviour of a 2-metre straw tracker, Tech. rep., CERN, Geneva, pH-EP-Tech-Note-2010-011 (2010).
- [6] J. M. Gere, Mechanics of Materials. Sixth edition., Tompson Learning, Inc, 2004.
- [7] V. Davkov, K. Davkov, V.V.Myalkovskiy, V. Peshekhonov, High pressure thin-wall drift tubes, Instrum. Exp. Tech. 51 (2008) 787–791. doi:10.1134/S002044120806002X.
- [8] S. Timoshenko, S. Woinowsky-Krieger, Theory of Plate and Shells, McGraw-Hill Book Co, International Edition, 1959.
- [9] D. C. Livio, Qualification of the longitudinal weld of thin wall pet tubes of the straw tracker of the na62 experiment, Master’s thesis, Haute Ecole Libre Mosane, Liege (2011).
- [10] MITSUBISHI POLYESTER FILM GmbH, Hostaphan RNK 2600 (2016).
URL https://www.m-petfilm.de/wp-content/uploads/RNK_2600e.pdf
- [11] J. Haringx, Instability of thin-walled cylinders subjected to internal pressure, Philips Research Reports 7 (1952) 112–118.
- [12] A. Palmer, J. Baldry, Lateral buckling of axially constrained pipelines, Journal of Petroleum Technology 26 (1974) 1283–1284. doi:10.2118/4815-PA.
- [13] L. Rayleigh, The Theory of Sound, Vol. 1, MacMillan and Co, Inc., London, 1894.
- [14] H. Fletcher, Normal vibration frequencies of a stiff piano string, The Journal of the Acoustical Society of America 36 (1964) 203–209.
- [15] Vishay Precision Group, Inc., Single-Point Aluminum Load Cell. Model 1022. Tedea-Huntleigh (2016).
URL <http://www.vishaypg.com/docs/12007/1022.pdf>
- [16] F. James, M. Roos, Minuit: A System for Function Minimization and Analysis of the Parameter Errors and Correlations, Comput. Phys. Commun. 10 (1975) 343–367. doi:10.1016/0010-4655(75)90039-9.

- [17] R. Brun, F. Rademakers, ROOT: An object oriented data analysis framework, Nucl. Instrum. Meth. A389 (1997) 81–86.
doi:10.1016/S0168-9002(97)00048-X.
- [18] Goodfellow Group of companies, Polyethylene terephthalate (2016).
URL <http://www.goodfellow.com/E/Polyethylene-terephthalate.html>

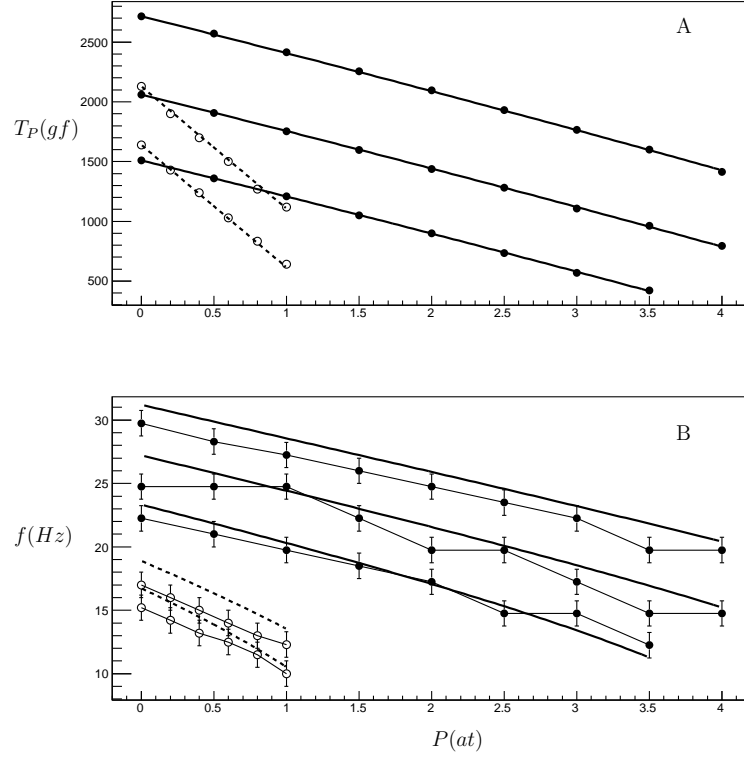


Figure 4: A: effective tensions T_P versus P for different initial tensions $T_P(0)$. B: lowest frequency for the corresponding P and T_P . Filled circles – 9.8-mm straw, open circles – 18-mm straw. Curves: formula (15) for the plot A and (12) for B; solid lines – 9.8-mm straw, dashed lines – 18-mm straw.

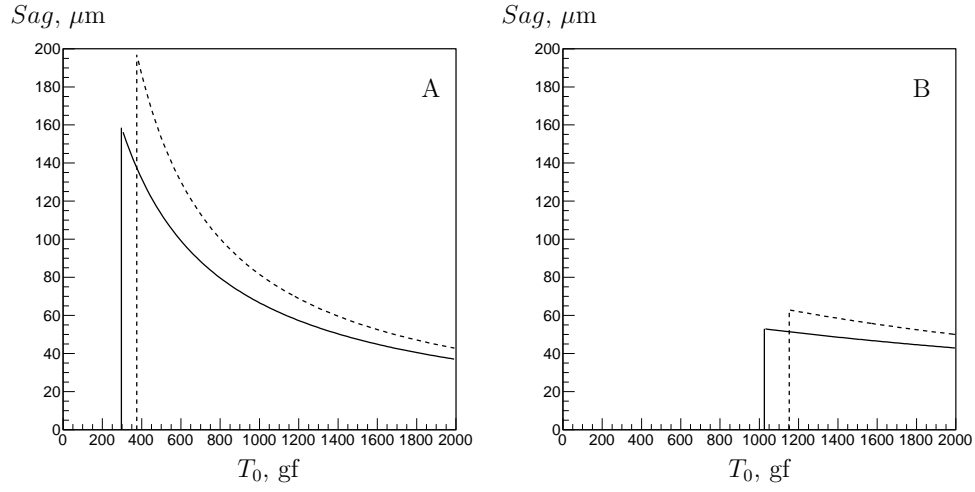


Figure 5: Sagitta in vacuum Sag versus pre-tension T_0 of 70-cm-long straw segment for 9.8-mm straw (A) and 18-mm straw (B). Vertical lines mark the buckling limit $T_P = 0$. Solid line is calculated for the central values for all the parameters. Dashed lines show the worst case (see text).